Supporting Information

Wang et al. 10.1073/pnas.1501441112

SI Materials and Methods

Animals. Adult male C57BL/6J mice (10–12 wk old) from the Jackson Laboratory and Chinese Academy of Sciences at Shanghai were housed in a temperature- and humidity-controlled animal facility with a 12-h light/dark cycle and freely available food and water. All experiments were approved by the University of Pittsburgh's and Fudan University's Institutional Animal Care and Use Committees and performed in accordance with the National Institutes of Health's *Guide for the Care and Use of Laboratory Animals* (1). Animal suffering and numbers killed were minimized to the greatest extent possible.

Randomization of Animal Grouping, Investigator Blinding, and Exclusion Criteria. Animal group assignments for TBI or sham operation, for treatment of Scriptaid or vehicle, or for neurobehavioral testing or sacrifice for brain assessments were done at random using a lottery-drawing box. All main outcome studies, including neurobehavioral tests, electrophysiology, lesion volume, histology, and immunohistochemistry, were performed by investigators blinded to group assignment and experimental conditions. Animals that died during or after surgery were excluded from the studies.

Animals were closely observed for the first 2 h after surgery, and then watched twice daily for the first 3 d and three times per week until sacrifice. Animals exhibiting one or more of the following signs were also excluded: (*i*) weight loss >20% of baseline weight. (with animals weighed before surgery and every day for the first 5 d after surgery.); (*ii*) moribund and unresponsive to external stimuli; (*iii*) inability to attend to normal physiological needs, such as eating, drinking, and grooming; and (*iv*) inability to ambulate.

TBI. TBI was induced by a CCI, as described previously (2, 3). In brief, all animals were assigned at random into experimental groups and anesthetized with 1.5% isoflurane in a 30% O_2/68.5% N_2O mixture under spontaneous breathing conditions. After a craniotomy was performed, the CCI was centered 2 mm lateral to midline and 1.0 mm anterior to bregma and produced with a pneumatically driven CCI device (Precision Systems and Instrumentation) using a 3-mm flat-tipped impounder (velocity, 3.5 m/s; duration, 150 ms; depth, 1.5 mm). The bone flap was then replaced and sealed. Rectal temperature was maintained at 37 °C ± 0.5 °C during surgery and for up to 30 min after TBI using a heating pad. Sham animals were subjected to all aspects of the surgery and handling except for CCI.

Drug Administration. Scriptaid (Sigma-Aldrich; CN: S7817) was stored as a 100-mg/mL stock solution in dimethyl sulfoxide (DMSO). As described previously (2), Scriptaid was diluted in sterile saline, heated to boiling, and cooled to 37 °C or lower before i.p. delivery. Immediately after surgery, animals were assigned at random to the vehicle or Scriptaid group using a lottery-drawing box. Vehicle control animals received a 0.5% DMSO solution in saline. Scriptaid was injected at 3.5 mg/kg at 2 h after CCI, and this was repeated daily for the next 2 d (at 26 and 50 h after injury).

Immunohistochemistry and Cell Counting. Brains were removed after fixative perfusion and cryoprotected in 30% sucrose in phosphate-buffered saline (PBS). Serial sections were cut on a freezing microtome, blocked, and incubated in the following primary antibodies: goat anti-CD206 (R&D Systems), rat anti-CD16/32 (BD), rabbit anti-MBP (Abcam), mouse anti-nonphosphorylated neurofilaments (SMI-32; Abcam), mouse anti-GSK3β (Cell Signaling Technology), and rabbit anti-Iba1 (Wako). Images were processed for automated analysis with ImageJ software (National Institutes of Health). Cell numbers were calculated per square millimeter from three random microscopic fields (200× magnification) on three sections (nine images total) cut through the CC (n = 6 animals per group). All counts were performed in a blinded fashion.

Fluorescence Quantification. Immunostaining was performed with rabbit anti-MBP and mouse anti-nonphosphorylated neurofilament (monoclonal antibody SMI-32 from Abcam, raised against an abnormally dephosphorylated epitope on 200-kDa neurofilament H). The immunostained CC area of TBI animals was contrasted with immunostaining in sham animals using confocal microscopy (FV1000; Olympus) and analyzed with ImageJ software. A region of interest (ROI) was drawn over the ipsilateral CC by a blinded investigator, and similar ROIs were drawn in sham animals. White matter damage was expressed as the ratio of SMI-32 to MBP immunostaining relative to sham animals.

Luxol Fast Blue Staining. Coronal sections (25 μm) were stained with Luxol fast blue according to the manufacturer's instructions (American Mastertech) to detect myelin damage. In brief, slides were incubated for 1 h in a preheated solution of Luxol fast blue (60 °C). After a water rinse, sections were differentiated in lithium carbonate solution for 30 s, followed by 70% ethyl alcohol for 30 s. The slides were then rinsed, and differentiation was verified under the microscope. After alcohol dehydration, the slides were coverslipped for microscopic examination.

Neurobehavioral Tests.

Rotarod test. The rotarod test was carried out as described previously (4). In brief, mice were placed on a rotating drum with speed accelerating from 4 to 40 rpm during a 5-min period. The time at which the animal fell off the drum was recorded. The test began 1 d before TBI and consisted of two trials. On the day of TBI, the animals underwent five trials, with the mean value from these trials serving as the presurgery baseline value for each animal. After surgery, animals were tested for five trials on a daily basis for up to 11 d.

Wire hang test. The wire hang test was performed as described previously (2). The experimental apparatus was a stainless steel bar (50 cm long, 2-mm diameter) resting on two vertical supports and elevated 37 cm above a flat surface. Mice were placed on the bar midway between the supports and were observed for 30 s in four trials. The amount of time spent hanging was recorded and scored according to the following criteria: 0, fell off; 1, hung onto the bar with two forepaws; 2, hung onto the bar with an added attempt to climb onto the bar; 3, hung onto the bar with two forepaws and one or both hind paws; 4, hung onto the bar with all four paws and with tail wrapped around the bar; 5, escaped to one of the supports.

CatWalk gait analysis. Gait abnormalities were measured using an automated computer-assisted method (CatWalk; Noldus Information Technology) according to the manufacturer's instructions, as described previously (5, 6). The analysis was performed in dark and silent room (<20 lx of illumination). In brief, mice were placed on an elevated 1.3-m-long and 0.68-m- wide glass plate illuminated sideways with fluorescent light internally reflected in the glass. When their paws contacted the glass plate, light left the glass plate owing to alterations in the refractive index. A camera and computer captured and analyzed the images of paw contacts. The home cage was placed at the end of the walkway as bait, and animals were trained to run toward this cage for three sessions

before the analysis. Locomotor speed was determined by dividing the covered distance on the walkway (20 cm) by the time taken for the animal to cross it. A minimum of three compliant runs were achieved, with a minimum duration of 0.5 s, maximum duration of 5 s, and maximum speed variation of 60%. If an animal turned or walked backward, the trial was excluded, and another was conducted.

The CatWalk system objectively measures various aspects of footfalls in a dynamic manner. Based on the position, pressure, and surface area of each footfall, multiple parameters were calculated automatically. In this study, we used the following parameters: (*i*) print area, the surface area (in square millimeters) of the complete print, including all frames that make up a stance; (*ii*) intensity, a parameter that reflects of the mean pressure exerted by a paw during the floor contact when crossing the walkway, with data presented as arbitrary units; and (*iii*) stance phase, duration (expressed in seconds) of the contact of a paw with the glass plate in each step cycle. One step cycle is the time between two consecutive initial contacts of the same paw and consists of the stance phase and swing phase (i.e., duration of no contact with the glass plate in a step cycle).

Real-Time PCR. Total RNA was isolated with the RNeasy Mini Kit (Qiagen) according to the manufacturer's instructions. The first strand of cDNA was synthesized from 5 μg of RNA with the SuperScript First-Strand Synthesis System (Invitrogen). RT-PCR was performed using the Opticon 2 Real-Time PCR Detection System (Bio-Rad) and SYBR gene PCR Master Mix (Invitrogen) as described previously (3, 7). Cycle time values were measured as a function of GAPDH mRNA levels in the same tissue. The sequences of the primer pairs for the M1 phenotype genes were as follows (in pairs, sense and antisense): iNOS: CAAGCACCTTGGAAGAGGAG and AAGGCCAAACACAGCATACC; CD16: TTTGGACACCCAGATGTTTCAG and GTCTTCCTTGAGCACCTGGATC. The sequences of the primer pairs for the M2 phenotype genes were as follows: CD206: CAAGGAAGGTTGGCATTTGT and CCTTTCAGTCCTTTGCAAGC; IL-10: CCAAGCCTTATCGGAAATGA and TTTTCACAGGGGAGAAATCG. Primer pairs against murine CK2α and GSK3β were as follows: CK2α: CATGCACAGGGATGTGAAAC and AGAATGGCTCCTTTCGGAAT; GSK3β: ACCAATATTTCCTGGGGACA and GTGCCTTGATTTGAGGGAAT.

CAP Measurements. CAPs in the CC and external capsule were measured as described previously (8). Coronal brain slices (350 μm thick, bregma −1.06 mm) were placed in pregassed (95% O_2/5% CO_2) artificial cerebrospinal fluid (aCSF; 126 mmol/L NaCl, 2.5 mmol/L KCl, 1 mmol/L $Na_2H_2PO_4$, 2.5 mmol/L $CaCl_2$, 26 mmol/L $NaHCO_3$, 1.3 mmol/L $MgCl_2$, 10 mol/L glucose; pH 7.4) for 1 h at room temperature, and then perfused with aCSF at a constant rate (3–4 mL/min) at 22 °C. A bipolar tungsten-stimulating electrode (intertip distance, 100 μm) was positioned across the CC at ∼0.9 mm lateral to the midline. A glass extracellular recording pipette (5–8 MΩ tip resistance when filled with aCSF) was placed in the external capsule, 0.24–0.96 mm from the stimulating electrode in 0.24-mm increments. Only the recording at 0.48 mm from the stimulating electrode is reported here. Both electrodes were placed 50–100 μm below the surface of the slice, with adjustments to optimize the signal (9). The CAP was amplified (× 1 k) and recorded using an Axoclamp 700B (Molecular Devices), and then analyzed using pCLAMP 10 software (Molecular Devices). Input–output curves were generated by varying the intensity of the stimuli from 0.05 mA to 0.55 mA in 0.05-mA increments (100-μs duration, delivered at 0.05 Hz) (10). Average waveforms of four successive sweeps in two slices per animal were analyzed. Myelinated fiber amplitude was defined as the difference from the first peak to the first trough (N1).

Primary Microglia and Oligodendrocyte Cultures. Primary microglia and oligodendrocytes were collected from mixed cultures harvested from 1-d-old postnatal mice, as described previously (7). LPS (100 ng/mL) or LPS plus IFN-γ (20 ng/mL) was added to microglia for 48 h for M1 induction. IL-4 (20 ng/mL) was added for 48 h for M2 induction (7). Oligodendrocytes were cultured in medium containing 15 nM triiodothyronine and 1 ng/mL ciliary neurotrophic factor. Two in vitro systems were used: a Transwell system allowing communication via diffusible factors and a simple CM transfer from microglial cultures to oligodendrocyte cultures (Fig. 3*A*). Oligodendrocytes were subjected to OGD for 2 h and then returned to normal medium for 24 h. Unstimulated, M1, or M2 microglia in Transwells were added on top of control or post-OGD oligodendrocytes in the lower chamber. In some experiments, the microglial CM was collected and added to the oligodendrocytes (at a 1:1 CM-to- oligodendrocyte culture medium ratio). The MTT assay for viability, LDH activity assay for loss of membrane integrity, and immunocytochemical staining for MBP were performed 24 h later.

Lentiviral shRNA Infection. Lentiviral shRNA directed at mouse GSK3β (sc-35525-V), mouse mTOR (sc-35410-V), and a lentivirus containing a control, nontargeting sequence of shRNA (sc-108080), with titers of $\sim 5 \times 10^3$ infectious units/μL, were purchased from Santa Cruz Biotechnology. Cells were transfected with 1.5 μL virus per well in six-well plates for 48 h, and knockdown of each protein was confirmed by Western blot analysis.

For intracerebral lentiviral shRNA infection, the viral particles containing shRNA for GSK3β or a nontargeting sequence were infused into the right CC (0.75 mm lateral to bregma, 0.82 mm posterior to bregma, and 1.75 mm ventral to skull) at 7 d before TBI. Viruses were infused at a rate of 0.1 μL/min over 50 min with a microinfusion system linked to a microsyringe pump (UMP2; World Precision Instruments), as described previously (11). To confirm that lentiviral vectors achieved efficient infection in CC, viral particles containing GFP were infused as described above. Lentivirus-mediated gene expression in mouse brains was verified 7 d later by the detection of GFP expression (Fig. S6*B*). The infusion of viral particles into the brain did not cause any increase in animal mortality.

Measurements of Cell Viability and Cell Death in Cultures. Metabolic viability in vitro was assessed with the MTT assay (3). Live cells were incubated with 1 g/L of MTT solution at 37 °C for 2 h. The medium was then carefully removed, and 100 μL of dimethylformamide was added into each well to dissolve the resultant dark-blue crystals for 1 h. Absorbance was measured at 570 nm (OD_{570}) with a universal microplate reader (Elx800; BioTek Instruments).

Alternatively, cell death was evaluated using the LDH assay for loss of membrane integrity and release of LDH into the culture medium. To perform this assay, aliquots of 100 μL were taken from culture medium and added to 150 μL of LDH reagent (Sigma-Aldrich). Absorbance of the reaction was assayed spectrophotometrically by monitoring the reduction of NAD^+ at 340 nm at 25 °C over a period of 5 min in the presence of lactate. Data were expressed as a percentage of the maximum LDH activity in control wells in which all cells were lysed with Triton (3).

Phagocytosis Assay. Microglia were plated at 1×10^5 cells/well in eight-well slides (Nunc; Thermo Scientific) as described previously (3, 7). Nile red fluorescent microspheres (0.03% solids; Invitrogen) were added to live cells for 3 h. For image analysis of phagocytosis, cells were rinsed in PBS three times, followed by fixation with 4% paraformaldehyde. Then Alexa Fluor 488 phalloidin (Invitrogen) was added for 1 h at room temperature in the dark. Images were obtained with an Olympus confocal microscope.

As a second measurement, microsphere fluorescence intensity was quantified by a plate reader as described previously (7). In

brief, cells were rinsed with PBS three times and then with 0.25 mg/mL trypan blue in PBS for 1 min to quench the signal from extracellular or outer plasma membrane-associated microspheres. Cells were then lysed using PBS with Tween 20 (1% Triton). Intracellular fluorescence of Nile red was measured using a fluorescence plate reader (excitation wavelength, 535 nm; emission wavelength, 575 nm).

Immunocytochemistry for MBP. Oligodendrocytes (non-OGD or post-OGD) cocultured with microglia were fixed and blocked for 1 h at 4 °C in 2% BSA in PBS with 0.5% Triton X-100. Cells were then incubated overnight at 4 °C with rabbit anti-MBP antibody (1:1,000) diluted in the same blocking solution. On the next day, cells were washed and incubated for 1 h at 4 °C with Alexa Fluor 488-conjugated goat anti-rabbit antibody (1:1,000; Jackson ImmunoResearch). After three more washes, nuclei were stained with DAPI. Immunostaining was visualized with an epifluorescent microscope.

Nuclear Protein Extraction. Nuclear protein extracts of primary microglia were prepared using the NE-PER nuclear and cytoplasmic extraction kit (Fisher Scientific), as described previously (2). Cells were washed with PBS and homogenized in a glass dounce homogenizer, followed by centrifugation at 500 × *g* for 5 min. The supernatant was removed from the pellet, and the pellet was resuspended in 400 μL of cytoplasmic extraction reagent I with protease inhibitors, followed by a 10-min incubation on ice. Subsequently, 22 μL of ice-cold cytoplasmic extraction reagent II were added to the sample before a 5-min centrifugation at 14,000 × *g*. The cytoplasmic extract in the supernatant was removed, and the nuclei-enriched pellet was resuspended in 200 μL of nuclear extraction reagent and then incubated on ice for 40 min. Following a final centrifugation at 14,000 × *g* for 10 min, the supernatant containing the nuclear protein extract was analyzed by Western blot analysis.

Western Blot Analysis. Cell lysates were run on SDS/PAGE gels, and proteins were detected on nitrocellulose blots with enhanced chemiluminescence reagents (GE Healthcare). The following antibodies were used: p-PTEN (Ser380/Thr382/383), PTEN, p-Akt (Ser473), Akt, p-mTOR (Ser2488), mTOR, p-GSK3β (Ser9), and GSK3β, all diluted 1:1,000 (Cell Signaling Technology), and p-PTEN (Ser385), p-PTEN (Ser370), and p-PTEN (Thr366), all diluted 1:500 (Millipore). Primary antibodies against acetylated H3, acetylated H4, total H3, and HDAC3 (Cell Signaling Technology) were used at 1:1,000 dilution. Membranes were blocked in 5% nonfat milk dissolved in Tris-buffered saline solution for 1 h, followed by overnight primary antibody incubation at 4 °C. On the next day, membranes were subjected to washing, followed by incubation with goat anti-rabbit IgG or goat anti-mouse IgG conjugated to horseradish peroxidase at a 1:1,000 dilution (Pierce Biotechnology) at room temperature for 1 h. Protein levels were analyzed by Scion Image and expressed as a fraction of β-actin or total H3 levels in the same lane.

Electron Microscopy. To visualize axonal damage in the CC, electron microscopy was performed as described previously (8). In brief, mice were perfused with saline, followed by ice-cold 4% paraformaldehyde and 0.1% glutaraldehyde in 0.1 mol/L PBS (pH 7.4). The CC near the site of contusion (as illustrated in Fig. 2*C*) was microdissected into ∼1-mm blocks and fixed in 2% glutaraldehyde for 24 h. Tissue was then rinsed in PBS and fixed in osmium tetroxide. Following serial dehydration in acetone, tissue was embedded in epon-araldite epoxy resin, cut at 60 nm, and examined using a JEOL JEM-1230 transmission electron microscope.

Because CCI results in both axonal damage and demyelination in the CC, we quantified the number of intact axons and the *g*-ratio using the methods described by Reeves et al. (12) and Chan et al. (13), respectively, with modifications. Two consecutive sections from each animal at the coronal level of anterior-posterior (AP) −1.06 from bregma were analyzed (n = 4/group). Three images (600 μm^2 each) at a magnification of 50,000× were acquired in randomly selected areas within the CC from each section and analyzed using ImageJ by an investigator blinded to experimental groups. Intact axons were defined using the three criteria described by Reeves et al. (12): (*i*) the membrane exhibited a continuous profile, (*ii*) the axoplasm contained at least one microtubule, and (*iii*) the axoplasm showed no degenerative debris. The *g*-ratio, an index of demyelination, was calculated for each intact axon using the following formula: *g*-ratio = axon diameter/axon diameter plus myelin thickness. At the coronal level of AP −1.06 from bregma, we found that unmyelinated axons constituted <5% of all axons within the CC in the sham control animals. Thus, the *g*-ratio was calculated based on all intact axons in the areas of interest.

HDAC Activity Assay. Nuclear extracts (20 μg) from the differently treated primary microglial cells were assayed for HDAC activity in triplicate using a colorimetric HDAC assay kit (Active Motif) according to the manufacturer's instructions and a previously published report (14). In this assay, when the acetylated substrate, BOC-(Ac)Lys-pNi-troanilide, is deacetylated, a colored product is generated with maximal absorption at 405 nm. Non-enzyme controls and positive controls using the HDAC inhibitor trichostatin A (TSA) were included as well.

Statistical Analyses. Data are presented as mean ± SEM. Differences between two groups were analyzed with the Student t test (two-tailed), and differences between multiple groups were analyzed with one-way ANOVA and the Bonferroni/Dunn post hoc test. Differences were considered significant at $P \leq 0.05$.

1. Committee on Care and Use of Laboratory Animals (1996) *Guide for the Care and Use of Laboratory Animals* (Natl Inst Health, Bethesda), DHHS Publ No (NIH) 85-23.
2. Wang G, et al. (2013) Scriptaid, a novel histone deacetylase inhibitor, protects against traumatic brain injury via modulation of PTEN and AKT pathway: Scriptaid protects against TBI via AKT. *Neurotherapeutics* 10(1):124–142.
3. Wang G, et al. (2013) Microglia/macrophage polarization dynamics in white matter after traumatic brain injury. *J Cereb Blood Flow Metab* 33(12):1864–1874.
4. Wang J, et al. (2014) Omega-3 polyunsaturated fatty acids enhance cerebral angiogenesis and provide long-term protection after stroke. *Neurobiol Dis* 68:91–103.
5. Hetze S, Römer C, Teufelhart C, Meisel A, Engel O (2012) Gait analysis as a method for assessing neurological outcome in a mouse model of stroke. *J Neurosci Methods* 206(1):7–14.
6. Neumann M, et al. (2009) Assessing gait impairment following experimental traumatic brain injury in mice. *J Neurosci Methods* 176(1):34–44.
7. Hu X, et al. (2012) Microglia/macrophage polarization dynamics reveal novel mechanism of injury expansion after focal cerebral ischemia. *Stroke* 43(11):3063–3070.
8. Pu H, et al. (2013) Omega-3 polyunsaturated fatty acid supplementation improves neurologic recovery and attenuates white matter injury after experimental traumatic brain injury. *J Cereb Blood Flow Metab* 33(9):1474–1484.
9. Reeves TM, Phillips LL, Lee NN, Povlishock JT (2007) Preferential neuroprotective effect of tacrolimus (FK506) on unmyelinated axons following traumatic brain injury. *Brain Res* 1154:225–236.
10. Kumar S, et al. (2013) Estrogen receptor β ligand therapy activates PI3K/Akt/mTOR signaling in oligodendrocytes and promotes remyelination in a mouse model of multiple sclerosis. *Neurobiol Dis* 56:131–144.
11. Stetler RA, et al. (2010) Apurinic/apyrimidinic endonuclease APE1 is required for PACAP-induced neuroprotection against global cerebral ischemia. *Proc Natl Acad Sci USA* 107(7):3204–3209.
12. Reeves TM, Smith TL, Williamson JC, Phillips LL (2012) Unmyelinated axons show selective rostrocaudal pathology in the corpus callosum after traumatic brain injury. *J Neuropathol Exp Neurol* 71(3):198–210.
13. Chan CB, et al. (2014) PIKE is essential for oligodendroglia development and CNS myelination. *Proc Natl Acad Sci USA* 111(5):1993–1998.
14. Meeran SM, Patel SN, Tollefsbol TO (2010) Sulforaphane causes epigenetic repression of hTERT expression in human breast cancer cell lines. *PLoS ONE* 5(7):e11457.
15. Ning K, et al. (2009) Leptin-dependent phosphorylation of PTEN mediates actin restructuring and activation of ATP-sensitive K^+ channels. *J Biol Chem* 284(14):9331–9340.

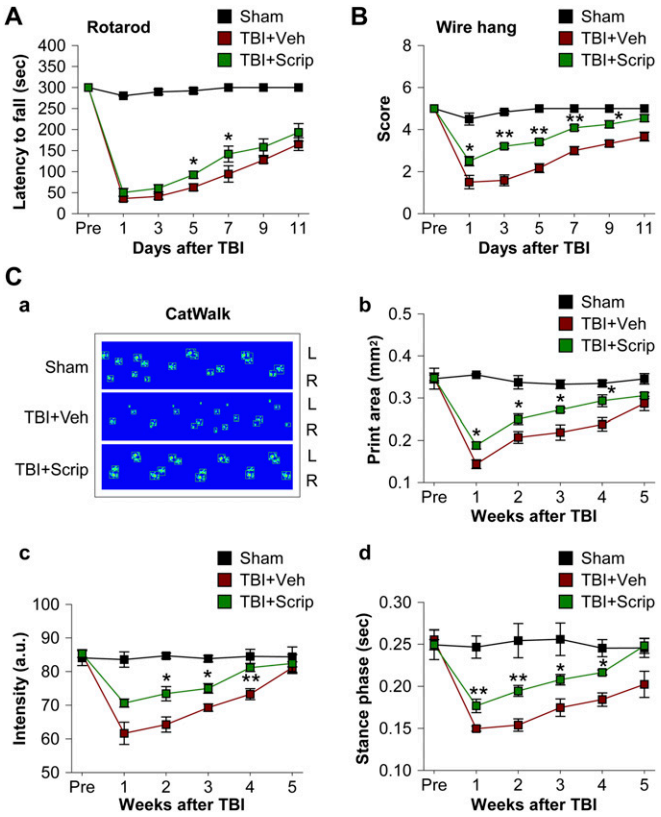

Fig. S1. HDAC inhibition improves sensorimotor functions of TBI mice in the CCI model. (*A* and *B*) Post-TBI treatment with the HDAC inhibitor Scriptaid improved the performance of TBI mice in the rotarod test (significantly improved at 5 and 7 d after TBI; *A*) and wire-hang test (significantly improved at 1, 3, 5, 7, and 9 d after TBI; *B*). (*C*) Post-TBI treatment with Scriptaid improved long-term sensorimotor performance on the CatWalk gait analysis. (*a*) Representative images of footfalls obtained by the CatWalk system at 1 wk after TBI in three experimental groups. All animals moved from left to right. The frame outside each footprint was generated automatically by the analysis system. TBI reduced the contact area of paws on both left (L, contralateral to the brain lesion) and right (R, ipsilateral to the brain lesion) sides, with the left side showing more severe impairment (*Middle*). The reduced print area was likely related to reduced limb weight-bearing after TBI, which was ameliorated in the Scriptaid-treated animals (*Lower*). (*b*) Summarized data on the area of the footfalls of the left hind paws. (*c*) Intensity (i.e., pressure exerted on the glass plate) of the left hind paws, in arbitrary units (a.u.). TBI-induced reductions in print area and intensity were partially restored with Scriptaid, suggesting protection of limb function and increased weight-bearing. (*d*) Stance phase of the left hind paws was measured as the period during which the left hind paw was in contact with the glass runway in a step cycle. Mice showed a reduced stance phase of the left hind paws after TBI, which may reflect reduced use of the paws on the injured side. Scriptaid treatment improved use of the injured limb by increasing the stance phase. Shown are the mean ± SEM values from 10–12 mice per group. $*P \leq 0.05$, $**P \leq 0.01$ vs. vehicle.

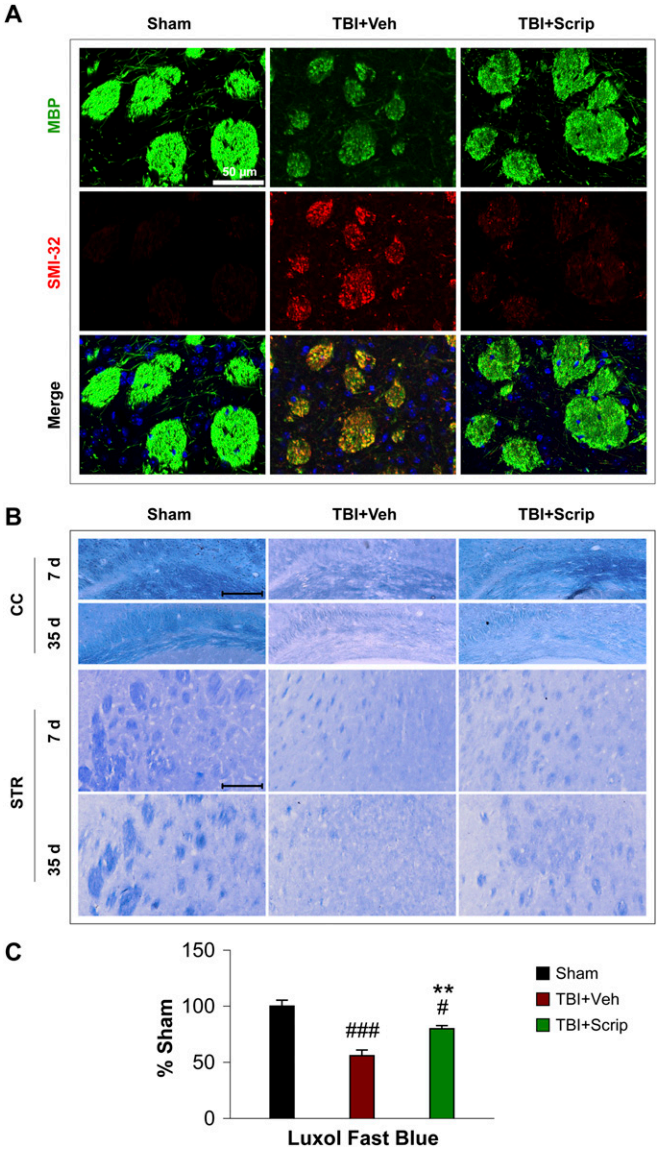

Fig. S2. Long-term attenuation of WMI by HDAC inhibition. (*A*) WMI was evaluated by double immunofluorescent staining for MBP and SMI-32 in the ipsilesional striatum at 35 d after TBI (vehicle and Scriptaid groups) or after sham surgery (sham group). As expected, SMI-32 immunoreactivity was rarely seen in normal-appearing white matter, and high MBP expression in the myelinated fiber bundles of the internal capsule was detected in sham-treated brains. Scriptaid decreased demyelination of white matter, as reflected in less neurofilament dissolution (i.e., less SMI-32 staining) and reduced loss of MBP. (*B*) Scriptaid reduced TBI-induced myelin loss in the CC and striatum (STR), as shown by the myelin-specific stain Luxol fast blue. (*C*) The integrated density of Luxol fast blue staining was quantified using ImageJ software and normalized to sham animals. Background staining was subtracted. Shown are the mean ± SEM values from six mice per group. $^{\#}P \leq 0.05$, $^{\#\#\#}P \leq 0.001$ vs. sham; $^{**}P \leq 0.01$ vs. vehicle.

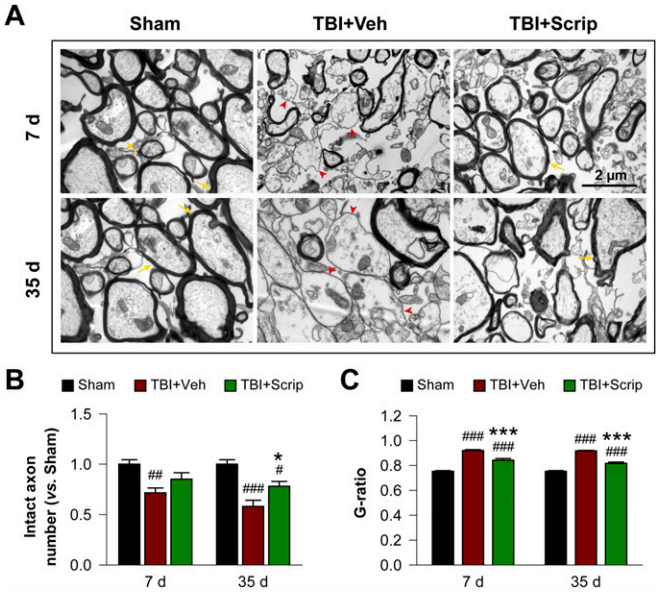

Fig. S3. HDAC inhibition preserves white matter ultrastructure after TBI. (*A*) Scriptaid reduced axonal demyelination in the CC, as visualized by transmission electron microscopy. In sham animals, closely packed myelinated axons (yellow arrows) were abundant. After CCI (TBI+Veh), many axons lost their myelin sheath (red arrows); mice treated with Scriptaid (TBI+Scrip) had more myelinated axons (yellow arrows). (*B* and *C*) Quantification of the numbers of intact axons per EM field (600 μm^2) (*B*) and the *g*-ratio (the ratio of axonal diameter to overall diameter of the axon plus myelin; *C*) in the CC at 7 d and 35 d after TBI or sham surgery. Vehicle-treated TBI mice had decreased numbers of intact axons per EM field and increased *g*-ratio compared with the sham controls; these changes were significantly attenuated in Scriptaid-treated TBI mice. Shown are the mean ± SEM values from four mice per group. $^{\#\#}P \leq 0.01$, $^{\#\#\#}P \leq 0.001$ vs. sham; $^{*}P \leq 0.05$, $^{***}P \leq 0.001$ vs. vehicle.

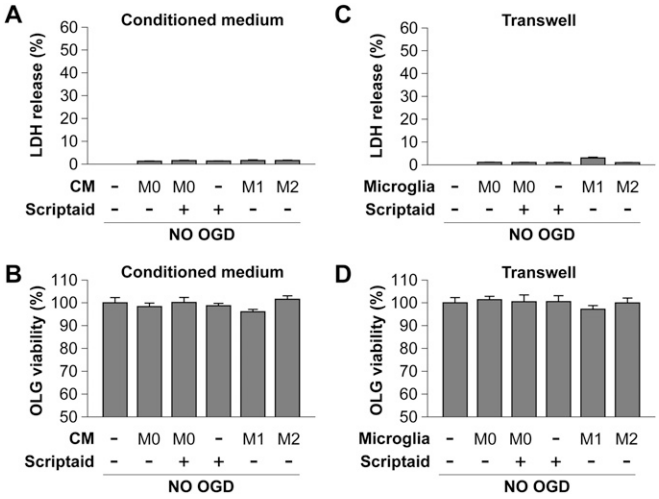

Fig. S4. Lack of effect of microglial phenotype on oligodendrocyte survival in control conditions (no OGD) in the in vitro experiments using a CM transfer system or a Transwell system (Fig. 3*A*). Cultured microglia (M0) were incubated with Scriptaid (1 μM) or vehicle for 48 h; as positive controls, microglia were primed toward M1 or M2 using LPS (100 ng/mL) plus IFN-γ (20 ng/mL) or IL-4 (20 ng/mL), respectively, for 48 h. Oligodendrocyte cultures were exposed to a 2-h control non-OGD condition (no OGD). After 24 h, microglia-CM or in-Transwell microglia were applied to oligodendrocyte cultures for 24 h. Cell death was quantified by LDH release (*A* and *C*) and MTT viability assays (*B* and *D*). Microglial phenotype did not affect oligodendrocyte cell viability in the absence of OGD. Shown are the mean ± SEM values from six independent experiments.

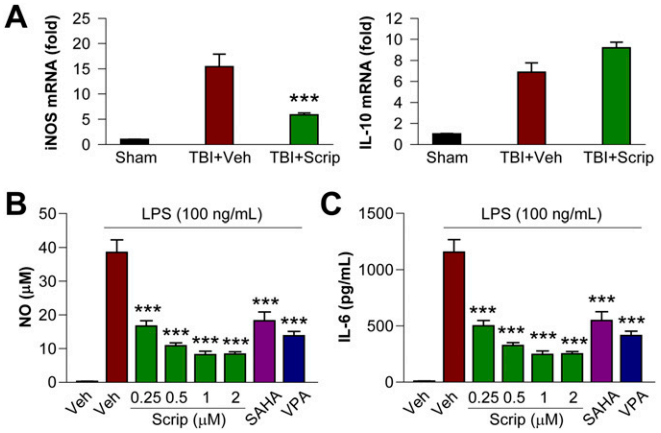

Fig. S5. HDAC inhibition reduces release of inflammatory mediators. (*A*) Messenger RNA levels of the M1 marker iNOS and the M2 marker IL-10 in the ipsilateral striatum at 7 d after TBI. (*B* and *C*) Cultured mouse primary microglia were challenged with LPS, and 1 h later, one of the HDAC inhibitors Scriptaid, SAHA (2.5 μM), or VPA (4 μM) were added to microglia. NO (*B*) and IL-6 (*C*) production was measured 24 h later. Shown are the mean ± SEM values from four independent experiments. ***$P \leq 0.001$ vs. LPS + vehicle.

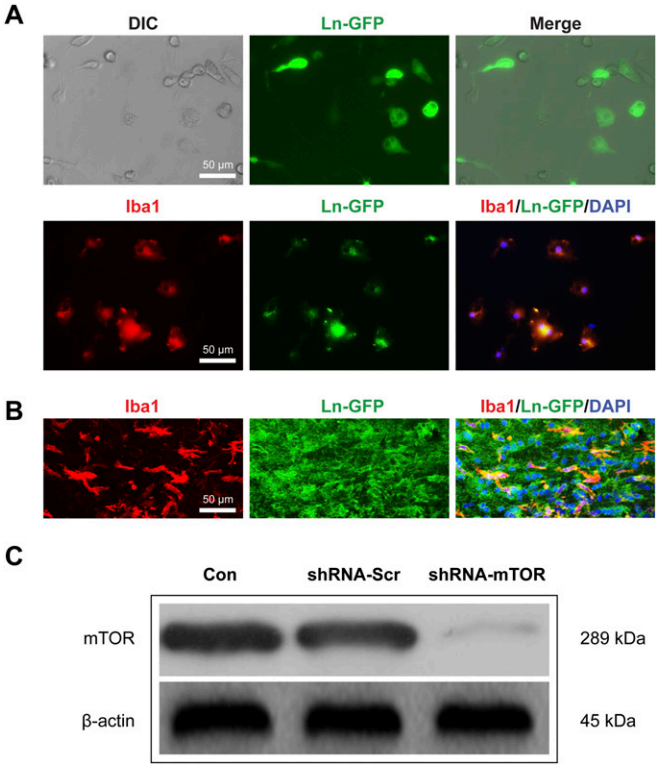

Fig. S6. Demonstration of lentivirus-mediated gene expression or knockdown in cultured microglial cells and in a mouse brain. (*A*) Primary mouse microglial cultures were infected with lentivirus bearing the GFP gene for 24 h, and then fixed and stained for the microglial marker Iba1 (red). Cells were visualized on a microscope with differential interference contrast and epifluorescent illumination. Nuclei were counterstained with DAPI (blue). (*B*) Lentiviral particles bearing the GFP gene were injected stereotaxically into the CC of mouse brain. At 7 d after vector injection, coronal sections through the CC were stained for Iba1 (red) and DAPI (blue) and viewed on an epifluorescent microscope. Lentiviral infection resulted in efficient gene transduction in primary mouse microglia and mouse brain, as shown by the colocalization of GFP with Iba1 (*A* and *B*, yellow). (*C*) Primary microglial cultures were infected with lentiviral vectors carrying shRNA targeting mTOR (shRNA-mTOR) or control scrambled sequences (shRNA-Scr). Knockdown of mTOR protein was confirmed by Western blot analysis at 72 h after lentiviral infection.

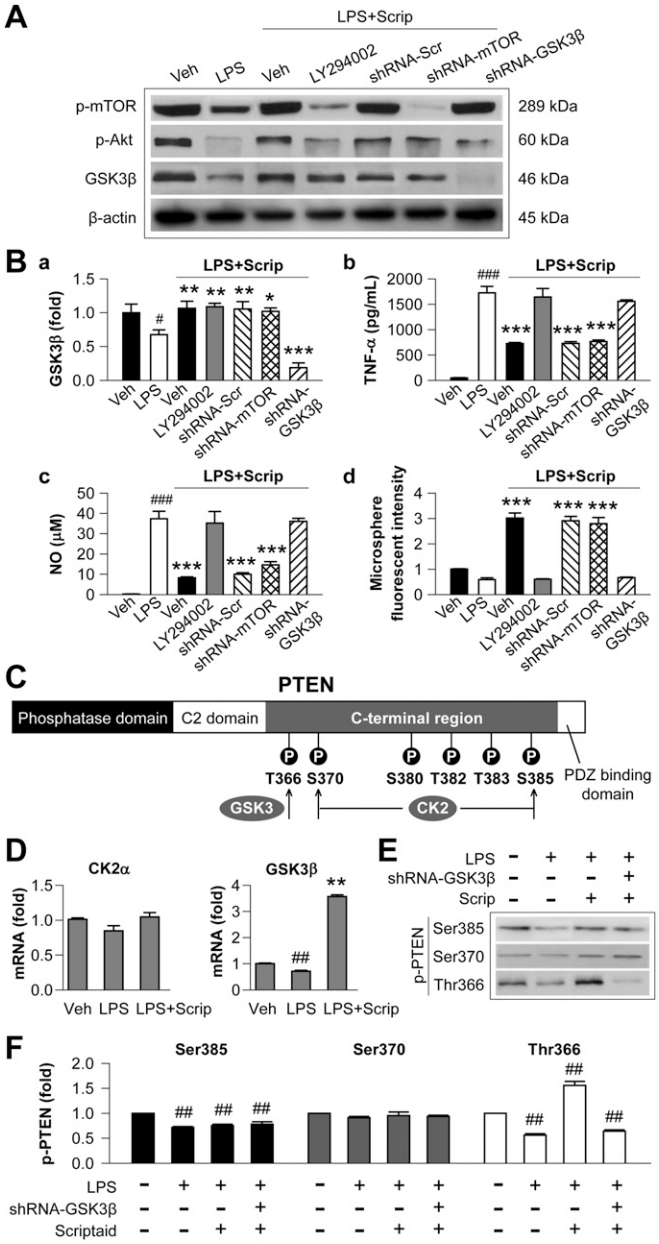

Fig. S7. The effects of HDAC inhibition on microglial polarization are mediated by GSK3β-dependent phosphorylation of PTEN. Cultured mouse primary microglia were transfected with lentivirus containing a scrambled sequence or shRNA targeting GSK3β or mTOR for 48 h, and then treated with LPS. Scriptaid was added to microglia at 1 h after LPS, and LY294002 was added at 5 min before Scriptaid. Two hours later (3 h after LPS treatment), protein and mRNA were harvested for Western blot analysis and RT-PCR, respectively. (*A*) Scriptaid prevented reduction of p-Akt, p-mTOR, and GSK3β in response to LPS, as determined by Western blot analysis. LY294002 reversed the impact of Scriptaid on p-Akt (Ser473) and p-mTOR (Ser2448), and GSK3β knockdown with lentiviral shRNA (shRNA-GSK3β) prevented the action of Scriptaid on p-Akt. m-TOR knockdown with lentiviral shRNA (shRNA-mTOR) had no effect on p-Akt or GSK3β. (*B*) Levels of GSK3β, TNF-α, NO, and phagocytic activity in LPS- and Scriptaid-treated microglia and the impact of LY294002 and m-TOR or GSK3β knockdown on these measures. LY294002 or m-TOR knockdown had no effect on GSK3β. LY29402 or GSK3β knockdown abolished the protective effects of Scriptaid against inflammatory markers and on phagocytosis. (*C*) The C-terminal domain of PTEN is illustrated with the main phosphorylation sites and their respective kinases. The schematic is based on work by Ashford et al. (15). (*D*) Real-time PCR for GSK3β and CK2 mRNA in primary microglia treated with LPS with or without Scriptaid. LPS reduced GSK3β mRNA levels, and Scriptaid markedly increased these levels. (*E* and *F*) Western blots using phosphorylation site-specific p-PTEN antibodies in LPS- and Scriptaid-treated microglia and the impact of GSK3β knockdown. Values are the mean ± SEM from four independent experiments. $^{\#}P \leq 0.05$, $^{\#\#}P \leq 0.01$, $^{\#\#\#}P \leq 0.001$ vs. vehicle; $^{*}P \leq 0.05$, $^{**}P \leq 0.01$, $^{***}P \leq 0.001$ vs. LPS alone.

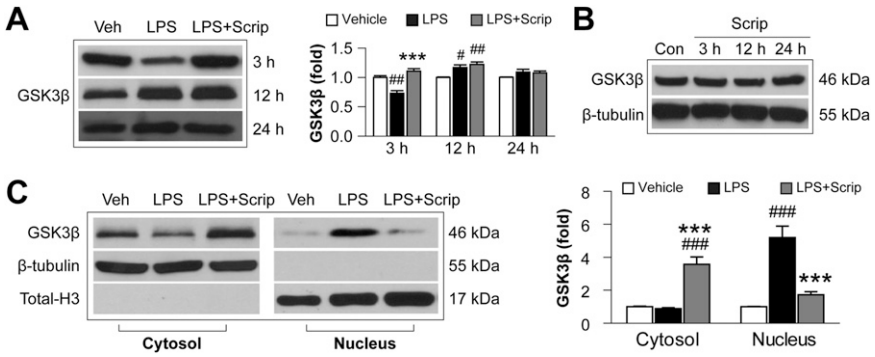

Fig. S8. HDAC inhibition modulates the spatiotemporal distribution of GSK3β in LPS-treated microglia. (*A*) Scriptaid prevented the acute loss of GSK3β in LPS-treated microglia at 3 h, but within 12 h of LPS treatment, LPS increased GSK3β expression. GSK3β levels returned to baseline within 24 h in all groups. (*B*) Scriptaid treatment by itself did not alter GSK3β expression in microglia within 24 h. (*C*) Western blot analysis of GSK3β expression in the cytosolic and nuclear fractions of microglia at 12 h after LPS stimulation. GSK3β was predominantly cytosolic in untreated microglia, but was decreased in the cytoplasm and increased in the nucleus after LPS stimulation. Scriptaid significantly increased cytosolic GSK3β expression relative to the control or LPS-only groups, and almost completely reversed the LPS-induced increase in nuclear GSK3β. Shown are the mean ± SEM values from four independent experiments. $^{\#}P \leq 0.05$, $^{\#\#}P \leq 0.01$, $^{\#\#\#}P \leq 0.001$ vs. vehicle; $^{***}P \leq 0.001$ vs. LPS group.